On Decomposition-Based Surrogate-Assisted Optimization of Leaky Wave Antenna Input Characteristics for Beam Scanning Applications

MEHMET ALI BELEN[ID][1]**, PEYMAN MAHOUTI**[ID][2]**,
SLAWOMIR KOZIEL**[ID][3,4]**, (Senior Member, IEEE),
ALPER ÇALIŞKAN**[5]**, AND STANISLAW SZCZEPANSKI**[ID][4]

[1]Department of Electrical and Electronic Engineering, İskenderun Technical University, 31200 Hatay, Turkey
[2]Department of Electronic and Communication, Vocational School of Technical Sciences, Istanbul University-Cerrahpasa, 34320 Istanbul, Turkey
[3]Engineering Optimization and Modeling Center, Department of Technology, Reykjavik University, 101 Reykjavik, Iceland
[4]Faculty of Electronics, Telecommunications and Informatics, Gdansk University of Technology, 80-233 Gdansk, Poland
[5]Department of Electronic and Communication Engineering, Yıldız Technical University, 34000 Istanbul, Turkey

Corresponding author: Slawomir Koziel (koziel@ru.is)

ABSTRACT Recent years have witnessed a growing interest in reconfigurable antenna systems. Travelling wave antennas (TWAs) and leaky wave antennas (LWAs) are representative examples of structures featuring a great level of flexibility (e.g., straightforward implementation of beam scanning), relatively simple geometrical structure, low profile, and low fabrication cost. Notwithstanding, the design process of TWAs/LWAs is a challenging endeavor because efficient handling of their electrical/field characteristics requires repetitive full-wave electromagnetic (EM) analyses, which is computationally expensive. In this paper, a novel approach to rapid optimization of LWA's input characteristics is proposed, based on structure decomposition and rendition of fast surrogate models of the antenna unit cells. The surrogates are combined into a single metamodel representing antenna input characteristics, which enables low-cost adjustment of the geometry parameters. The presented methodology is demonstrated through the design of several LWAs operating in the frequency bands of 8.2 GHz to 11.2 GHz, 6.2 GHz to 8.2 GHz, and 3.8 GHz to 4.7 GHz. Numerical results are validated through physical measurements of the fabricated array prototype.

INDEX TERMS Reconfigurable antenna, leaky wave antennas, beam scanning, EM-driven design, surrogate modeling, decomposition.

I. INTRODUCTION

Reconfigurable structures have been drawing considerable attention in the context of high-performance wireless communication system design. This is primarily due to their ability to adapt functionality to the operating conditions or system requirements [1]. Reconfigurable devices such as filters, couplers, junctions, and antennas [2]–[9], belong to the most efficient solutions for improving wireless communication system performance. In the case of antennas, reconfigurability is understood as the ability of altering the electrical and/or field properties such as operating frequency, polarization,

The associate editor coordinating the review of this manuscript and approving it for publication was Wen-Sheng Zhao[ID].

or pattern. It has become a key feature for many applications, including satellite and mobile communications [10], [11], digital television broadcasting [12], wearable devices [13], and radar [14]–[16]. Therein, a highly desirable feature is beam direction control, which can be realized either through electronic beam steering (to point the radiation direction at a desired angle at a single frequency), or frequency tunability, i.e., maintaining the beam direction over a range of frequencies [17].

Reconfigurability can be implemented in traveling wave antennas (TWAs), which utilize the traveling wave phenomenon along the guiding structure as the main radiating mechanism. TWA designs are based on the traditional microstrip array antennas as proposed by Menzel

in 1979 [18]. Their advantages include simple topology, low profile, and easy impedance matching [19]. Traveling wave antennas fall into two categories, slow-wave and fast-wave antennas. The fast-wave structures are usually referred to as leaky-wave antennas (LWAs) [20], [21]. In a slow-wave antenna, the wave propagates with a phase velocity lower than the speed of light in the free space, and the radiation only occurs at discontinuities, typically, the feed and the termination regions [20]. Obtaining a highly-directive single-beam radiation pattern is therefore difficult. By contrast, in LWAs, the wave phase velocity is greater than the speed of light, and this type of wave radiates continuously along the antenna length [20]. LWA usually consists of periodical structures whose geometry parameters have strong effects on the radiation characteristic. By using this type of antennas, it is possible to achieve highly-directive beams with low side lobe levels at an arbitrary specified angle. The wave phase constant, which can be altered by the operating frequency, allows for controlling the beam angle. This unique feature of LWA has been used for implementing high-performance pattern-reconfigurable antennas for beam scanning applications [22]–[28].

Notwithstanding, design of LWAs—that includes tuning of geometry parameters—is a challenging task, especially when stringent performance requirements concerning high gain, broadband operation without failing into open stop band (one of the drawbacks of LWAs that are due to coupling of a pair of oppositely-directed space harmonics; the latter results in most of the incident power being reflected, leading to a significant drop of the radiated power [29], [30]), and reconfigurability are to be satisfied. A dilemma is to conduct the design at the level of reliable EM-simulation model which incurs considerable computational costs, often prohibitive, or to work with lower-fidelity representations, which shortens the design cycle at the expense of the accuracy. A practical workaround is utilization of surrogate modelling techniques [31], [32], which preserves retaining reliability while retaining computational efficiency. Unfortunately, data-driven modelling of LWAs is difficult due to a typically large number of geometry parameters, and high cost of antenna simulation. This paper proposes a novel approach to optimization of input characteristics of LWAs, which capitalizes on the periodicity of the antenna structure, its decomposition, and incorporation of smaller-scale surrogates of the LWA unit cells, which are then combined into the overall metamodel using circuit theory rules. Thus, instead of using traditional transmission-line-equation-based calculation, which tends to differ from EM simulations and experimental results, data driven based surrogate modelling techniques are used to predict the behaviour of the unit elements. For the sake of demonstrating the flexibility of the approach, three LWA designs operating at different frequency bands have been obtained. Design reliability has been validated both numerically and experimentally. The proposed approach can be considered a rapid alternative to conventional (both direct and surrogate-assisted) LWA optimization techniques, and
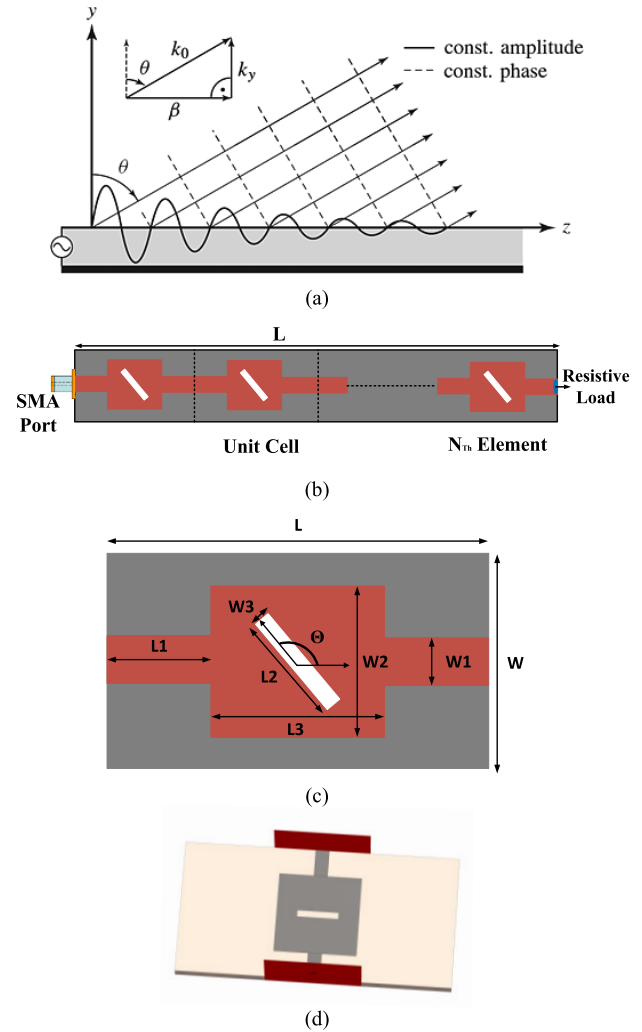

FIGURE 1. Open-end LWA: (a) conceptual illustration of LWA [33], (b) LWA Array, (c) Unit Element, (d) 3D EM model of unit element, designs considered in this work.

constitute a step towards design automation of leak-wave antennas.

II. CASE STUDY: OPEN-END LEAKY WAVE ANTENNA

Leaky-wave antennas (LWAs) typically consist of open-ended lines connected to ground. In these architectures, the radiating characteristic is mainly controlled by a travelling wave on a guiding structure, with the surface current being a superposition of electromagnetic waves traveling in the opposite directions [19]. A conceptual illustration of LWA has been shown in Fig. 1(a) [33].

LWAs are usually implemented as periodical structures. Figure 1(b) shows a geometry of a specific LWA proposed in this work. It is a cascade connection of unit patch elements presented in Fig. 1(c). Also 3D EM model of the unit element is presented in Fig. 1(d), where the unit element design is being fed using two waveguide ports. Its computational model contains ∼270,000 mesh cells. The average simulation time for unit element is around 15 seconds with
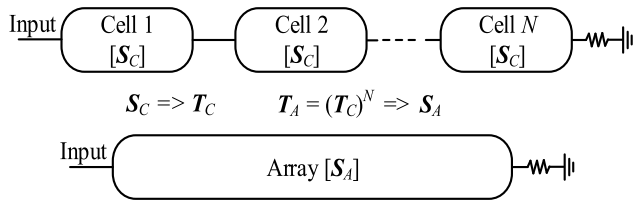
FIGURE 2. Conceptual illustration of the proposed LWA design methodology. The array is decomposed into unit cells represented by their S-parameter matrices. The transmission matrix of the array is computed by cascading the T-matrices of the cell, which allows for yielding the S-matrix of the array. To accelerate the design process, the matrix SC is represented by a fast data-driven surrogate model.

the following hardware setup: AMD Ryzen 7 3700X CPU @ 3.6 GHz with 16 GB installed memory on a 64-bit operating system.

Some of important design considerations of LWAs are: (i) the overall gain is monotonically related to the number of array elements, (ii) increasing the number of elements improves impedance matching, (iii) the operating band is mainly effected by the substrate height, patch widths, and material permittivity, (iv) increasing the antenna length allows for achieving a wider range of scanning at the expense of enlarging the array size, (v) with a proper selection of a periodical unit element design, an appropriate impedance matching can be achieved for suppression of the open stop band [29], [30] which becomes one of the main challenges in design optimization process. Notwithstanding, the main design factor is determination of the optimal dimensions of the unit element. This can only be achieved through rigorous EM-based optimization, which is a computationally expensive endeavour. The primary objective of this paper is to propose an efficient surrogate-assisted approach to rapid optimization of LWA's reflection characteristics, as described in Section III.

III. DESIGN METHODOGY
This section introduces a methodology of fast optimization of input characteristics of LWAs proposed in this work. The outline of the main concept is followed by a description of the unit element modeling procedure and array optimization.

A. LWA DESIGN BY DECOMPOSITION AND SURROGATE MODELLING
The LWA design methodology proposed in this paper is based on array decomposition and incorporation of fast data-driven surrogate models. As indicated in Fig. 2, the unit cells are represented by their corresponding S-matrices $\boldsymbol{S}_C$. The S-matrix $\boldsymbol{S}_A$ (Eq. 2) of the LWA is obtained from the transmission matrix $\boldsymbol{T}_A$ obtained by cascading the T-matrices of the unit cells, i.e., $\boldsymbol{T}_A = (\boldsymbol{T}_C)^N$. The major acceleration factor is that—for design optimization purposes—the matrix $\boldsymbol{S}_C$ is a parameterized data-driven surrogate obtained from sampled EM-simulation data of the unit cell, which enables rapid parameter adjustment of the LWA.

TABLE 1. Parameter ranges of unit cell surrogate model in Figure 1(c).

Parameter	Range	Step size
L_1 (mm)	[2.0 , 10.0]	0.5
W_1 (mm)	[2.0 , 4.0]	0.5
L_3 (mm)	[5.0 , 30.0]	2.0
Frequency (GHz)	[1.0 , 15.0]	0.1

The transformation of the unit cell S-matrix into the corresponding cell transmission matrix follows the standard two-port network rules. We have

$$T_C = \begin{bmatrix} T_{C.11} & T_{C.12} \\ T_{C.21} & T_{C.22} \end{bmatrix}$$
$$= \begin{bmatrix} \dfrac{S_{C.12}S_{C.21} - S_{C.11}S_{C.22}}{S_{C.21}} & \dfrac{S_{C.11}}{S_{C.21}} \\ \dfrac{-S_{C.22}}{S_{C.21}} & \dfrac{1}{S_{C.21}} \end{bmatrix} \quad (1)$$

where subscript C specified that the above matrices are pertinent to the unit cell. As mentioned before, the transmission matrix of the array is obtained by cascading the transmission matrices of N cells, i.e., we have

$$\boldsymbol{T}_A = (\boldsymbol{T}_C)^N \quad (2)$$

Finally, the S-matrix of the array is obtained by the transformation inverse to (1), i.e.,

$$S_A = \begin{bmatrix} S_{A.11} & S_{A.12} \\ S_{A.21} & S_{A.22} \end{bmatrix}$$
$$= \begin{bmatrix} \dfrac{T_{A.12}}{T_{A.22}} & \dfrac{T_{A.11}T_{A.22} - T_{A.12}T_{A.21}}{T_{A.22}} \\ \dfrac{1}{T_{A.22}} & \dfrac{-1}{T_{A.22}} \end{bmatrix} \quad (3)$$

where the subscript A specifies the matrices of the array.

B. UNIT CELL MODELLING
For the purpose of surrogate modeling, the flexibility offered by the original parameterization of the unit element is excessive, therefore, the following constraints are introduced: $W_2 = L_3$, $W_3 = L_2/2$, $L_2 = L_3/2$, $\theta = 90°$. Consequently, we have three independent parameters, L_1, W_1, and L_3. The data samples are allocated using a grid sampling as described in Table 1. It should be noted that the parameter ranges are very broad (the average upper-to-lower bound ratio is as high as seven), which is to ensure that the LWA can be designed over wide ranges of operating frequencies. The substrate parameters are $\varepsilon_r = 3$ and $h = 1.5$ mm. EM simulation of the unit element is then carried out to extract the S parameters. The dataset is split into the training (80%) and holdout (20%) parts.

The surrogate is constructed as a Multi-layer perceptron (MLP) [34], which is one of the commonly used Artificial Neural Network (ANN) regression models, proved to be suitable for modeling of high-frequency components [1], [32].

Model identification is carried out to minimize mean absolute error estimated using K-fold cross-validation (here, $K = 4$) [35]. Due to the reciprocal characteristic of the unit cell ($S_{ij} = S_{ji}$, $i, j = 1, 2$), and the substrate material represented as lossless material in the computational model, by modelling S_{11} characteristic the $\boldsymbol{S}_C$ matrix of the unit cell can be obtained at the expense of having a slight difference with experimental results, which will be discussed in Section IV.

C. ARRAY OPTIMIZATION

Having a fast surrogate, the LWA is optimized with respect to the parameter vector $\boldsymbol{x} = [L_1 \ W_1 \ L_3]^T$, by solving

$$\boldsymbol{x}^* = \arg \min_{\boldsymbol{x}} H(\boldsymbol{x}) \tag{4}$$

where the objective function is defined as

$$H(\boldsymbol{x}) = \max \{f \in [f_{c1}, f_{c2}] : |S_{11}(\boldsymbol{x}, f)|\} \tag{5}$$

where explicit dependence of S_{11} on $\boldsymbol{x}$ has been marked. Thus, (4), (5) is a minimax task oriented towards minimizing the array reflection response within the target operating frequency range from f_{c1} to f_{c2}.

Due to broad ranges of geometry parameters, utilization of a global search algorithm is instrumental in identifying the optimum design. On the other hand, as the surrogate model evaluation cost is negligible as compared to the cost of EM analysis, the employment of nature-inspired algorithms is feasible. Here, we use Honey Bee Mating Optimization (HBMO), which is a population-based metaheuristic algorithm [36].

The flowchart of the complete design methodology has been shown in Fig. 3.

IV. RESULTS AND EXPERIMENTAL VALIDATION

This section provides simulation and experimental verification of the design methodology presented in Section III. We start by validating the unit cell surrogate, which is constructed using MLP with 2 hidden layers containing 15 and 30 neurons, respectively, and trained using the Levenberg-Marquardt back-propagation algorithm [37]. The hold-out performance of the MLP model is evaluated based on two error metrics: Mean absolute Error(MAE) and Relative Mean Error (RME). The numerical data is presented in Table 2, whereas Fig. 4 shows the surrogate and EM-simulated unit cell responses at the selected testing location.

It can be observed that both error metrics are low, and the visual agreement between the surrogate-predicted cell outputs and EM simulation data is satisfactory. Consequently, the model can be employed for constructing the decomposition surrogate and rapid dimensioning of the LWA.

In order to demonstrate flexibility and re-usability of the presented approach, three different LWA designs have been obtained by optimizing the decomposition-based surrogate. The design task (3)-(4) has been solved using the
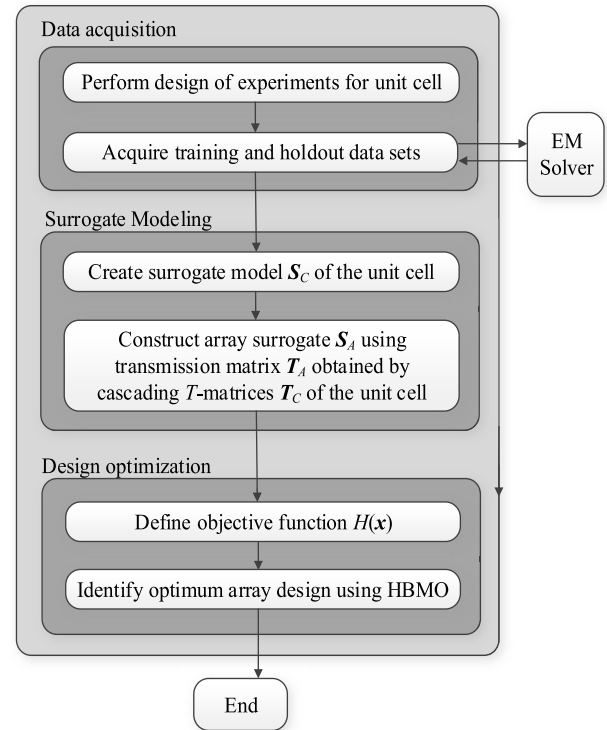
FIGURE 3. Flowchart of the proposed surrogate-assisted decomposition-based LWA design methodology.

TABLE 2. Performance of MLP surrogate model for holdout dataset.

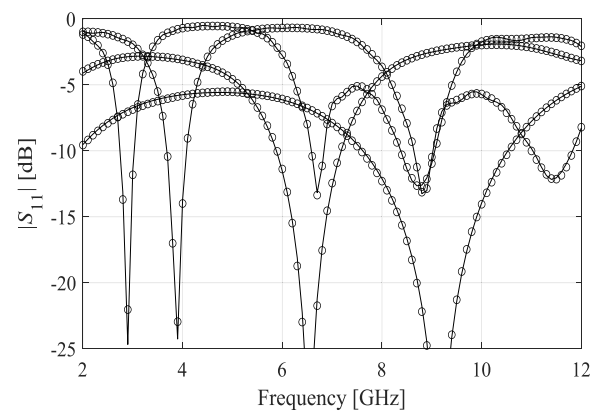| Parameter	MAE	RME
Magnitude $|S_{11}|$	$4.6 \ 10^{-3}$	2.1%
Phase of S_{11}	5.4	2.9%

FIGURE 4. Visualization of the data-driven surrogate model (o) versus EM simulation data (—) for selected testing points. The observed visual alignment of the two data sets is excellent.

HBMO algorithm as mentioned in Section III *C*. The target operating frequencies for the said designs are:
- Design I: $f_{c1} = 8$ GHz, $f_{c2} = 12$ GHz;
- Design II: $f_{c1} = 6$ GHz, $f_{c2} = 8$ GHz;
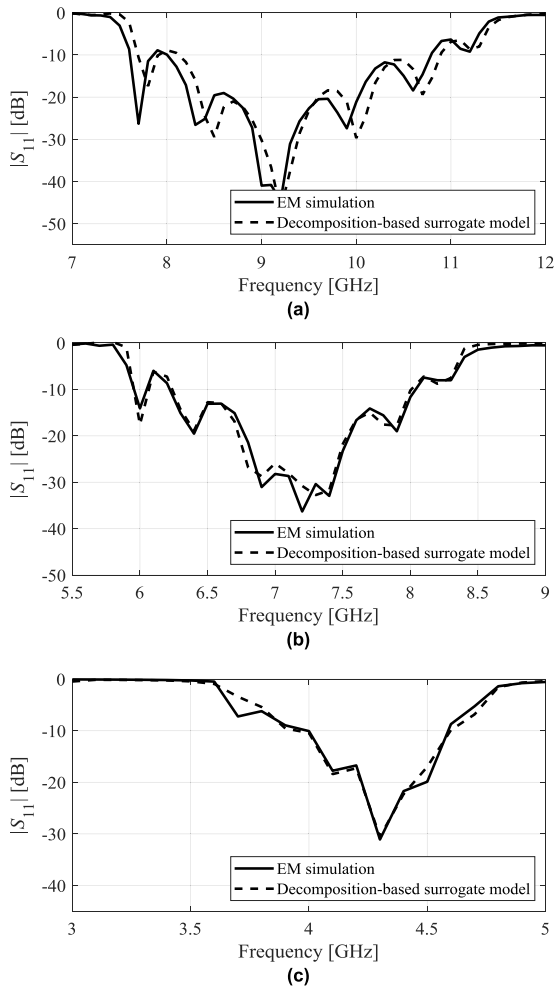- Design III: $f_{c1} = 4$ GHz, $f_{c2} = 4.5$ GHz.

TABLE 3. Radiation characteristics of LWA design 1 through 3.

Operating frequency [GHz]	Realized Gain [dBi]	Beam Scanning [Degree]	Array size [mm]
8.2-11.2	2.5-11	-66 ~ -6	95×30
6.2-8.2	2.2-10.5	-67 ~ -10	120×30
3.8-4.7	5.0-11	-65 ~ -5.0	207×20

FIGURE 5. Fig. 5. Visualization of the data driven surrogate model performance for optimized 7 element LWA designs with geometrical design parameters of (a) Design I [L1 = 2.2, W1 = 3.2, L3 = 8.6], (b) Design II [L1 = 3.1, W1 = 3.0, L3 = 10.9], (c) Design III [L1 = 5.8, W1 = 2.5 L3 = 18.0].

FIGURE 6. Decomposition-based surrogate model and measured characteristics of LWA Design I [L1 = 2.2, W1 = 3.2, L3 = 8.6]: (a) antenna prototype, (b) simulated and measured reflection response, (c) comparison of reflection responses with and without losses as well as SMA connector included into the computational model.

Figure 5 shows the reflection response of the LWAs, as predicted by the surrogate model and EM analysis. The agreement between the two data sets is good, especially for Designs II and III. A slight frequency shift can be observed for Design I, which can be attributed to residual mutual coupling effects not taken into account by the surrogate (the issue to be address in the future work). Table 3 gathers the major performance figures of the considered designs, whereas Fig. 7 shows the radiation characteristics for Design I. A broad beam scanning range of up to 60 degrees should be noted.

For the sake of supplementary validation, Design I has been fabricated and experimentally validated using a 9 kHz-to-13.5 GHz Vector Network Analyzer, and LB-8180-NF broadband 0.8-to-18 GHz horn antenna, available in of Yildiz Technical University. The LWA has been implemented on Arlon AD300 substrate (ε_r = 3.0, h = 1.52 mm). The measured LWA performance can be found in Fig. 6 and Table 4.

TABLE 4. Measured/simulated characteristic of LWA design 1.

Operating frequency [GHz]	Realized Gain [dBi]	Main Beam Direction [Degrees]	$|S_{11}|$ [dB]
8.2	2.9/2.5	−63/−66	−14.6/−11.7
9	5.2/4.9	−44/−50	−20.7/−30.2
10	7.1/7.4	−25/−27	−10.9/−28.7
11.2	10.3/11.0	−8/−6	−7.9/−8.7

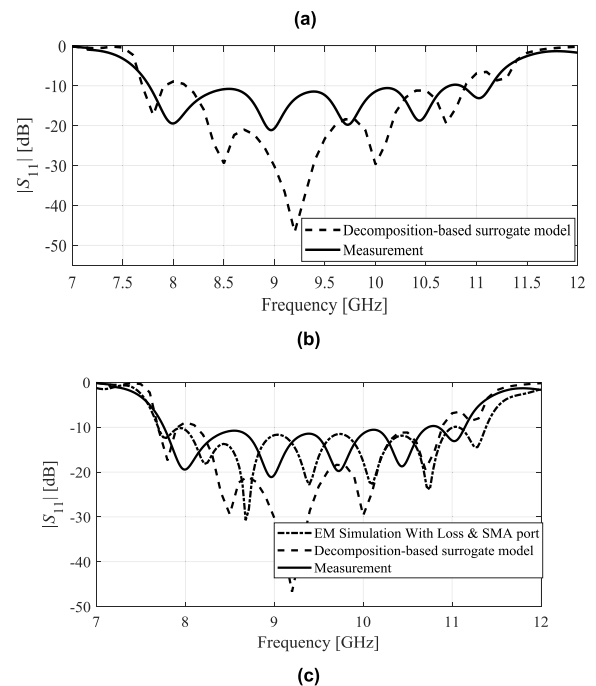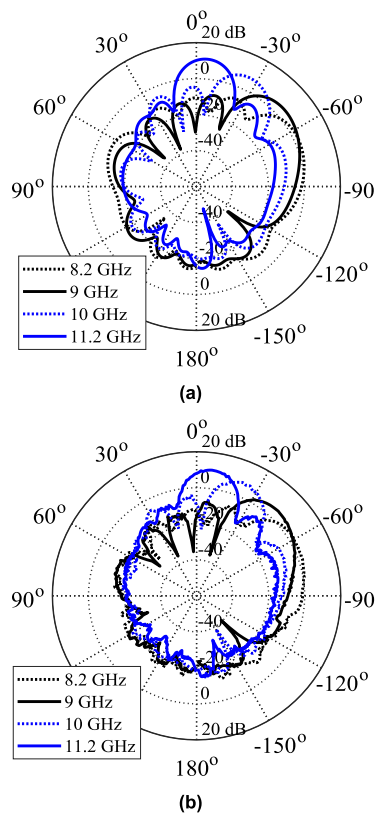It can be observed that the measured LWA performance is in a reasonably good agreement with the predictions

FIGURE 7. Decomposition-based surrogate model and measured characteristics of LWA Design I [L1 = 2.2, W1 = 3.2, L3 = 8.6]: (a) antenna prototype: (a) realized gain (simulation), (d) realized gain (measurement).

Work	f [GHz]	Scan Angle Range [Degrees]	Peak Gain [dBi]	Length
This work	8.2-11.2	-63 to -8	10.3	$3.1\,\lambda_0$
[19]	8-14	-65 to 15	12	$4.3\lambda_0$
[39]	9-14	-40 to 35	12	$5.46\lambda_0$
[40]	12.5-15.4	0 to 28	13.17	$13.8\lambda_0$
[41]	11.3-15.8	-60 to 38	15	$5.4\lambda_0$
[42]	11 -17.5	-85 to 85	10.7	$12\,\lambda_0$
[43]	17.5-19	0 to 60	-	$4\,\lambda_0$
[44]	5.6-6	79 to 103	8.89	$4.2\,\lambda_0$
[45]	10.7-18	-78 to 27	16	$8.44\,\lambda_0$
[46]	10-17.5	-49 to 69	14.2	8.3
[47]	8.4-14.4	-51 to 36	15	$8.6\lambda_0$

Furthermore, Table 5 provides performance comparison with state-of-the-art designs [19], [39]–[47]. As it can be observed, although the radiation performance of the considered LWA is inferior compared to some of the designs reported therein, it should be noted that the size of the array of Fig. 6 is 25 percent smaller than the design of [43], which features a similar scanning range of 60 degrees at the lower operating band, and almost twice as small in size compared to most of the arrays in Table 5. At the same time, the benchmark arrays employ considerably more complex unit elements that involve Substrate Integrated Waveguide (SIW) [39], [40], [44], [46], Dielectric Image Line (DIL) [41], or Composite Right Left Hand (CRLH) [42].

The radiation performance of the design can be improved by increasing the array size, which would also enable beam scanning from the backward quadrant to the forward quadrant and make the design perform better scanning range than most of the benchmark designs. Still, in this work, the major focus is on optimization of input characteristics. In particular, the presented optimization approach can be applied to any a design with arbitrary number of unit elements, e.g., to ensure improved radiation characteristics.

The results discussed in this section demonstrate suitability of the methodology proposed in this work for rapid parameter tuning of LWAs over broad ranges of operating conditions. The decomposition-based surrogate provides reliable representation of the LWA reflection characteristic, and—once established— can be reused without incurring any additional computational expenses. At the same time, the proposed technique only addresses optimization of input characteristics. Its generalization that includes handling of radiation patterns and mutual coupling will be given in the future work.

V. CONCLUSION
This paper introduced a technique for rapid optimization of input characteristics of leaky-wave antennas. Our methodology involved a decomposition-based surrogate, which capitalizes on the periodicity of the array topology.

obtained through EM simulations. Slight discrepancies can be attributed to manufacturing and assembly inaccuracies, but also neglecting losses within the unit elements. Clearly, experimental verification accounts for conductor (ohmic), dielectric and radiation losses, which can be reduced by using properly selected substrate materials [38] such as Arlon AD300, utilized in this work. Another modelling parameter that might contribute to the differences between simulation and experimental results is the feeding configuration. The unit element used in the considered demonstration example is configured with ideal waveguide port, whereas the measured design is fed through the SMA connectors. As it can be seen from Fig. 6(b), EM analysis results that incorporate the SMA connectors and material losses are better aligned with the measures results. However, the computational cost of the model including these is considerably higher (almost 2,900,000 mesh cells, simulation time ~13 minutes for the hardware setup mentioned before). Furthermore, as it can be seen from the results, with optimal selection of geometrical parameters of the unit cell designs, an impedance matching for the suppression of the open stop band has been achieved. Thus, the proposed method can be used not only for computationally efficient surrogate modelling but it can also be used to realize stop band suppression within the limits of unit element and array design for the selected operation bands.

An accurate data-driven model of the array unit cell is composed, using circuit theory rules, into a fast model of the entire array, which can be then optimized at negligible cost, even when using global search procedures. The proposed approach has been demonstrated through the design of three LWAs operating at different frequency bands (8.2 GHz to 11.2 GHz, 6.2 GHz to 8.2 GHz, and 3.8 GHz to 4.7 GHz) by reusing the same surrogate model. A good agreement between the array characteristics predicted by the surrogate and EM-simulated ones has been observed. The selected design corresponding to the operating bandwidth of 8.2 GHz to 11.2 GHz has been fabricated and measured to additionally corroborate the design utility of the presented procedure.

The future work will be focused on generalizations of the presented technique, first, to allow modeling of the array radiation patterns, and, furthermore, to account for mutual coupling effects. The latter is particularly important in the context of design of physically-reduced LWA layouts.

REFERENCES

[1] P. Mahouti, "Design optimization of a pattern reconfigurable microstrip antenna using differential evolution and 3D EM simulation-based neural network model," *Int. J. RF Microw. Comput.-Aided Eng.*, vol. 29, no. 8, p. e21796, Apr. 2019, doi: 10.1002/mmce.21796.

[2] X. Zhu, T. Yang, P.-L. Chi, and R. Xu, "Novel reconfigurable filtering rat-race coupler, branch-line coupler, and multiorder bandpass filter with frequency, bandwidth, and power division ratio control," *IEEE Trans. Microw. Theory Techn.*, vol. 68, no. 4, pp. 1496–1509, Apr. 2020.

[3] D. Psychogiou, "Reconfigurable all-pass-to-bandstop acoustic-wave-lumped-element resonator filters," *IEEE Microw. Wireless Compon. Lett.*, vol. 30, no. 8, pp. 745–748, Aug. 2020.

[4] M. Fan, K. Song, L. Yang, and R. Gómez-García, "Frequency-reconfigurable input-reflectionless bandpass filter and filtering power divider with constant absolute bandwidth," *IEEE Trans. Circuits Syst. II, Exp. Briefs*, vol. 68, no. 7, pp. 2424–2428, Jul. 2021.

[5] G. Monti, R. D. Paolis, and L. Tarricone, "Design of a 3-state reconfigurable CRLH transmission line based on MEMS switches," *Prog. Electromagn. Res.*, vol. 95, pp. 283–297, 2009.

[6] J. Ren, Z. Zhou, Z. H. Wei, H. M. Ren, Z. Chen, Y. Liu, and Y. Z. Yin, "Radiation pattern and polarization reconfigurable antenna using dielectric liquid," *IEEE Trans. Antennas Propag.*, vol. 68, no. 12, pp. 8174–8179, Dec. 2020.

[7] X. Yang, Y. Liu, H. Lei, Y. Jia, P. Zhu, and Z. Zhou, "A radiation pattern reconfigurable Fabry–Pérot antenna based on liquid metal," *IEEE Trans. Antennas Propag.*, vol. 68, no. 11, pp. 7658–7663, Nov. 2020.

[8] H. Sun, Y. Hu, R. Ren, L. Zhao, and F. Li, "Design of pattern-reconfigurable wearable antennas for body-centric communications," *IEEE Antennas Wireless Propag. Lett.*, vol. 19, no. 8, pp. 1385–1389, Aug. 2020.

[9] C. Fan, B. Wu, Y. Hu, Y. Zhao, and T. Su, "Millimeter-wave pattern reconfigurable Vivaldi antenna using tunable resistor based on graphene," *IEEE Trans. Antennas Propag.*, vol. 68, no. 6, pp. 4939–4943, Jun. 2020.

[10] P. Liu, W. Jiang, S. Sun, Y. Xi, and S. Gong, "Broadband and low-profile penta-polarization reconfigurable metamaterial antenna," *IEEE Access*, vol. 8, pp. 21823–21831, 2020.

[11] I. Serhsouh, M. Himdi, H. Lebbar, and H. Vettikalladi, "Reconfigurable SIW antenna for fixed frequency beam scanning and 5G applications," *IEEE Access*, vol. 8, pp. 60084–60089, 2020.

[12] A. N. Kulkarni and S. K. Sharma, "Frequency reconfigurable microstrip loop antenna covering LTE bands with MIMO implementation and wideband microstrip slot antenna all for portable wireless DTV media player," *IEEE Trans. Antennas Propag.*, vol. 61, no. 2, pp. 964–968, Feb. 2013.

[13] S.-J. Ha and C. W. Jung, "Reconfigurable beam steering using a microstrip patch antenna with a U-slot for wearable fabric applications," *IEEE Antennas Wireless Propag. Lett.*, vol. 10, pp. 1228–1231, 2011.

[14] Y. Liu, W. Zhang, Y. Jia, and A. Wu, "Low RCS antenna array with reconfigurable scattering patterns based on digital antenna units," *IEEE Trans. Antennas Propag.*, vol. 69, no. 1, pp. 572–577, Jan. 2021.

[15] J. Yu, W. Jiang, and S. Gong, "Low-RCS beam-steering antenna based on reconfigurable phase gradient metasurface," *IEEE Antennas Wireless Propag. Lett.*, vol. 18, no. 10, pp. 2016–2020, Oct. 2019.

[16] K. Kandasamy, B. Majumder, J. Mukherjee, and K. P. Ray, "Low-RCS and polarization-reconfigurable antenna using cross-slot-based metasurface," *IEEE Antennas Wireless Propag. Lett.*, vol. 14, pp. 1638–1641, 2015.

[17] E. Abdo-Sánchez, D. Palacios-Campos, C. Frías-Heras, F. Y. Ng-Molina, and T. M. Martín-Guerrero, "Electronically steerable and fixed-beam frequency-tunable planar traveling-wave antenna," *IEEE Trans. Antennas Propag.*, vol. 64, no. 4, pp. 1298–1306, Apr. 2016.

[18] W. Menzel, "A new travelling-wave antenna in microstrip," *AEU Int. J. Electron. Comm*, vol. 33, no. 4, pp. 137–140, 1979.

[19] F. Güneş, A. Belen, and M. A. Belen, "Microstrip tapered traveling wave antenna for wide range of beam scanning in X- and Ku-bands," *Int. J. RF Microw. Comput.-Aided Eng.*, vol. 29, no. 9, p. e21771, Sep. 2019.

[20] F. Frezza, "Introduction to traveling-wave antennas," *Eur. School Antennas*, pp. 1–10, 2006.

[21] A. Sutinjo, M. Okoniewski, and R. H. Johnston, "Radiation from fast and slow traveling waves," *IEEE Antennas Propag. Mag.*, vol. 50, no. 4, pp. 175–181, Aug. 2008.

[22] D. Comite, S. K. Podilchak, P. Baccarelli, P. Burghignoli, A. Galli, A. P. Freundorfer, and Y. M. M. Antar, "Design of a polarization-diverse planar leaky-wave antenna for broadside radiation," *IEEE Access*, vol. 7, pp. 28672–28683, 2019.

[23] Y. Zhang, H. Liu, C. Meng, Y. Lin, Y. Zhang, E. Forsberg, and S. He, "A broadband high-gain circularly polarized wide beam scanning leaky-wave antenna," *IEEE Access*, vol. 8, pp. 171091–171099, 2020.

[24] Q. Yang, X. Zhao, and Y. Zhang, "Design of CRLH leaky-wave antenna with low sidelobe level," *IEEE Access*, vol. 7, pp. 178224–178234, 2019.

[25] X. Li, J. Wang, Z. Li, Y. Li, M. Chen, and Z. Zhang, "Dual-beam leaky-wave antenna array with capability of fixed-frequency beam switching," *IEEE Access*, vol. 8, pp. 28155–28163, 2020.

[26] A. Iftikhar, M. Ur-Rehman, M. F. Shafique, U. Farooq, M. S. Khan, S. M. Asif, A. Fida, B. Ijaz, M. N. Rafique, and M. J. Mughal, "Planar SIW leaky wave antenna with electronically reconfigurable E- and H-plane scanning," *IEEE Access*, vol. 7, pp. 171206–171213, 2019.

[27] Y. Lin, H. Liu, Y. Zhang, E. Forsberg, and S. He, "A simple high-gain millimeter-wave leaky-wave slot antenna based on a bent corrugated SIW," *IEEE Access*, vol. 8, pp. 91999–92006, 2020.

[28] W. Ma, W. Cao, S. Shi, and X. Yang, "Compact high gain leaky-wave antennas based on substrate integrated waveguide TE220 mode," *IEEE Access*, vol. 7, pp. 145060–145066, 2019.

[29] J. T. Williams, P. Baccarelli, S. Paulotto, and D. R. Jackson, "1-D combline leaky-wave antenna with the open-stopband suppressed: Design considerations and comparisons with measurements," *IEEE Trans. Antennas Propag.*, vol. 61, no. 9, pp. 4484–4492, Sep. 2013.

[30] W. Zhou, J. Liu, and Y. Long, "Investigation of shorting vias for suppressing the open stopband in an SIW periodic leaky-wave structure," *IEEE Trans. Microw. Theory Techn.*, vol. 66, no. 6, pp. 2936–2945, Jun. 2018.

[31] P. M. Watson, K. C. Gupta, and R. L. Mahajan, "Development of knowledge based artificial neural network models for microwave components," in *IEEE MTT-S Int. Microw. Symp. Dig.*, Baltimore, MD, USA, Jun. 1998, pp. 9–12.

[32] A. Suntives, M. S. Hossain, J. Ma, R. Mittra, and V. Veremey, "Application of artificial neural network models to linear and nonlinear RF circuit modeling," *Int. J. RF Microw. Comput.-Aided Eng.*, vol. 11, no. 4, pp. 231–247, 2001.

[33] A. Ishimaru, *Electromagnetic Wave Propagation, Radiation, and Scattering*. Upper Saddle River, NJ, USA: Prentice-Hall, 1991.

[34] H. Taud and J. Mas, "Multilayer perceptron (MLP)," in *Geomatic Approaches for Modeling Land Change Scenarios* (Lecture Notes in Geoinformation and Cartography), O. M. Camacho, M. Paegelow, J. F. Mas, and F. Escobar, Eds. Cham, Switzerland: Springer, 2018.

[35] M. W. Browne, "Cross-validation methods," *J. Math. Psychol.*, vol. 44, no. 1, pp. 108–132, 2000.

[36] F. Güneş, S. Demirel, and P. Mahouti, "Design of a front–end amplifier for the maximum power delivery and required noise by HBMO with support vector microstrip model," *Radioengineering*, vol. 23, no. 1, pp. 134–143, 2012.

[37] X. Fu, S. Li, M. Fairbank, D. C. Wunsch, and E. Alonso, "Training recurrent neural networks with the Levenberg–Marquardt algorithm for optimal control of a grid-connected converter," *IEEE Trans. Neural Netw. Learn. Syst.*, vol. 26, no. 9, pp. 1900–1912, Sep. 2015.

[38] L. G. Maloratsky and M. Lines, "Reviewing the basics of microstrip," *Microw. RF*, vol. 39, pp. 79–88, Mar. 2000.

[39] Y.-L. Lyu, X.-X. Liu, P.-Y. Wang, D. Erni, Q. Wu, C. Wang, N.-Y. Kim, and F.-Y. Meng, "Leaky-wave antennas based on noncutoff substrate integrated waveguide supporting beam scanning from backward to forward," *IEEE Trans. Antennas Propag.*, vol. 64, no. 6, pp. 2155–2164, Jun. 2016.

[40] D. Lee and S. Lim, "Leaky-wave antenna design using quarter-mode substrate-integrated waveguide," *Microw. Opt. Technol. Lett.*, vol. 57, no. 5, pp. 1234–1236, May 2015.

[41] C. S. Prasad, A. Biswas, and M. J. Akhtar, "Leaky wave antenna for wide range of beam scanning through broadside in dielectric image line environment," *Microw. Opt. Technol. Lett.*, vol. 60, no. 7, pp. 1707–1713, Jul. 2018.

[42] S. Yan and Y. C. Li, "Design of broadband leaky-wave antenna based on permeability-negative transmission line," *Microw. Opt. Technol. Lett.*, vol. 60, no. 3, pp. 699–704, Mar. 2018.

[43] A. Kandwal, Q. Zhang, R. Das, X. Tang, and L. W. Louis, "Model analysis of coupled-mode leaky-wave antenna for forward and backward frequency scanning," *Microw. Opt. Technol. Lett.*, vol. 60, no. 6, pp. 1360–1368, Jun. 2018.

[44] M. Farooq, M. U. Khan, and H. M. Cheema, "A 5 GHz narrow-beam leaky-wave antenna using binomially distributed slot based substrate integrated waveguide," *Microw. Opt. Technol. Lett.*, vol. 60, no. 9, pp. 2288–2293, Sep. 2018.

[45] A. K. Tiwari, S. Awasthi, and R. K. Singh, "A symmetrical periodic leaky-wave antenna with backward-to-forward scanning," *IEEE Antennas Wireless Propag. Lett.*, vol. 19, no. 4, pp. 646–650, Apr. 2020.

[46] R. Ranjan and J. Ghosh, "SIW-based leaky-wave antenna supporting wide range of beam scanning through broadside," *IEEE Antennas Wireless Propag. Lett.*, vol. 18, no. 4, pp. 606–610, Apr. 2019.

[47] D. K. Karmokar, S.-L. Chen, D. Thalakotuna, P.-Y. Qin, T. S. Bird, and Y. J. Guo, "Continuous backward-to-forward scanning 1-D slot-array leaky-wave antenna with improved gain," *IEEE Antennas Wireless Propag. Lett.*, vol. 19, no. 1, pp. 89–93, Jan. 2020.

MEHMET ALI BELEN received the Ph.D. degree in electronics and communication engineering from the Yıldız Technical University, in 2016. He is currently an Associate Professor with İskenderun Technical University. His current research interests include multivariable network theory, device modeling, computer aided microwave circuit design, monolithic microwave integrated circuits, antenna arrays, and active/passive microwave components, especially in the field of metamaterial-based antennas and microwave filters.

PEYMAN MAHOUTI received the M.Sc. and Ph.D. degrees in electronics and communication engineering from Yıldız Technical University, Turkey, in 2013 and 2016, respectively. He is currently an Associate Professor with the Department of Electronic and Communication, Istanbul University-Cerrahpasa, Turkey. The main research areas are analytical and numerical modeling of microwave devices, optimization techniques for microwave stages, and application of artificial intelligence-based algorithms. His research interests include analytical and numerical modeling of microwave and antenna structures, surrogate-based optimization, and application of artificial intelligence algorithms.

SLAWOMIR KOZIEL (Senior Member, IEEE) received the M.Sc. and Ph.D. degrees in electronic engineering from the Gdansk University of Technology, Poland, in 1995 and 2000, respectively, and the M.Sc. degree in theoretical physics, the M.Sc. degree in mathematics, and the Ph.D. degree in mathematics from the University of Gdansk, Poland, in 2000, 2002, and 2003, respectively. He is currently a Professor with the Department of Engineering, Reykjavik University, Iceland. His research interests include CAD and modeling of microwave and antenna structures, simulation-driven design, surrogate-based optimization, space mapping, circuit theory, analog signal processing, evolutionary computation, and numerical analysis.

ALPER ÇALIŞKAN received the Ph.D. degree in electronics and communication engineering from Yıldız Technical University, in 2019. He is currently a Research Assistant with Yıldız Technical University. His main research interests include optimization of microwave and millimeter wave antennas, ultra wideband antennas, radar systems, and computer aided circuit design.

STANISLAW SZCZEPANSKI received the M.Sc. and Ph.D. degrees in electronic engineering from the Gdańsk University of Technology, Poland, in 1975 and 1986, respectively. In 1986, he was a Visiting Research Associate with the Institut National Polytechnique de Toulouse (INPT), Toulouse, France. From 1990 to 1991, he was with the Department of Electrical Engineering, Portland State University, Portland, OR, USA, on a Kosciuszko Foundation Fellowship. From August 1998 to September 1998, he was a Visiting Professor with the Faculty of Engineering and Information Sciences, University of Hertfordshire, Hatfield, U.K. He is currently a Professor with the Department of Microelectronic Systems, Faculty of Electronics, Telecommunications and Informatics, Gdańsk University of Technology. He has published more than 160 articles and holds three patents. His teaching and research interests include circuit theory, fully integrated analog filters, high-frequency transconductance amplifiers, analog integrated circuit design, and analog signal processing.

• • •